

Thermally Stimulated Luminescence Properties of Dy-doped $\text{Sr}_3\text{Gd}(\text{PO}_4)_3$ Single Crystals

Haruaki Ezawa,^{1*} Takumi Kato,¹ Yuma Takebuchi,² Kai Okazaki,¹ Kensei Ichiba,¹
Daisuke Nakauchi,¹ Noriaki Kawaguchi,¹ and Takayuki Yanagida¹

¹Division of Materials Science, Nara Institute of Science and Technology (NAIST), Ikoma, Nara 630-0192, Japan

²Faculty of Engineering, Utsunomiya University, Utsunomiya, Tochigi 321-8585, Japan

(Received September 24, 2024; accepted December 11, 2024)

Keywords: floating zone method, single crystals, Dy, thermally stimulated luminescence, dosimetric properties

In this study, we synthesized 0.1, 0.5, and 1% Dy-doped $\text{Sr}_3\text{Gd}(\text{PO}_4)_3$ single crystals using a floating zone furnace to evaluate their thermally stimulated luminescence (TSL) properties. In the TSL glow curve, two glow peaks appeared at around 80 and 110 °C in all the Dy-doped samples. In TSL spectra, all the Dy-doped samples showed emission peaks at 480, 580, 670, and 760 nm. The emission peaks were typical for the $4f-4f$ transitions of Dy^{3+} ions. After exposure to 1 Gy of X-ray radiation, the 0.5% Dy-doped sample demonstrated a spatial resolution of 56.2 μm .

1. Introduction

Storage-type phosphors, such as dosimetric materials, have the capability to temporarily store absorbed radiation energy. Owing to this capability, they are used in imaging plates and personal and environmental dosimetry.^(1–4) When exposed to radiation, dosimetric materials generate numerous electron-hole pairs. Some of them are stored in trapping centers and can later be re-excited by external stimulation. Once re-excited, they move to luminescent centers and recombine to emit photons.⁽⁵⁾ The type of stimulus determines the luminescence process: thermally stimulated luminescence (TSL) and optically stimulated luminescence (OSL).^(2,6–8) High luminescence intensity, low fading, and excellent thermal and chemical stabilities are key characteristics required for dosimetric materials. However, no dosimetric materials perfectly satisfy all the required characteristics. Thus, the development of new dosimetric materials is necessary.

$\text{Sr}_3\text{Gd}(\text{PO}_4)_3$ (SGPO) belongs to the group of disordered crystal materials known as $M_3RE(\text{PO}_4)_3$ (M : Sr or Ba element; RE : rare-earth elements). The materials have special qualities such as high mechanical and chemical stabilities, good optical quality, mild conductivity, and ease of obtaining large single crystals for mass manufacturing.^(9–14) Rare-earth-doped SGPO has gained attention lately because of its possible use as a phosphor. According to the results of

*Corresponding author: e-mail: ezawa.haruki.ec6@ms.naist.jp
<https://doi.org/10.18494/SAM5431>

experiments, SGPO shows good performance as a phosphor in laser and white LED applications.^(15,16) Therefore, SGPO would be a suitable candidate for dosimetric materials.

Over the past few decades, a variety of dosimetric materials in many material forms have been investigated, such as powders, ceramics, glasses, and single crystals.^(2,7,8,17–22) In general, single crystals are more transparent than ceramics. Therefore, photons are emitted from both the inner and outer surfaces of single crystals, and single crystals can exhibit a high luminescence intensity. As far as we know, ours is the only study on the TSL properties of SGPO single crystals. In our previous paper, nondoped and Tb-doped SGPO single crystals were synthesized, and their TSL properties were assessed.⁽²³⁾ Following this previous work, in this study, using the floating zone (FZ) method, SGPO single crystals doped with 0.1, 0.5, and 1% Dy were fabricated. Since Dy³⁺ ions are widely used in commercial TSL dosimeters, such as CaF₂,^(24,25) Dy-doped SGPO single crystals could be a candidate for a novel dosimetric material.

2. Materials and Methods

Different concentrations of Dy (0.1, 0.5, and 1% in relation to Gd) were doped to the host material. SrCO₃ (99.99%, Wako Pure Chemical), NH₄H₂PO₄ (99.99%, SIGMA-ALDRICH), Dy₂O₃ (99.99%, Furuuchi Chemical), and Gd₂O₃ (99.99%, Furuuchi Chemical) were used as raw powders. The synthesis method was the same as that for Tb-doped SGPO, and the FZ furnace (Crystal Systems Corporation, FZ-T-12000-X-VPO-PC-YH) was used.⁽²⁶⁾ As the growth conditions, a pull-down rate of 10 mm/h and a rotation rate of 20 rpm were used.

After the fabrication, some of the prepared single crystals were polished using a polishing device (Buehler, MetaServ 250). The polished single crystals were used to evaluate TSL properties. The single crystals that were unpolished were used for powder X-ray diffraction (XRD) measurements using an X-ray diffractometer (Rigaku, MiniFlex600).

The samples were exposed to X-rays from an X-ray generator (Spellman, XRB80N100/CB) prior to measurements of TSL glow curves and spectra, and X-ray imaging. The samples were heated using a temperature controller/power supply (Sakaguchi E.H Voc, SCR-SHQ-A), and the TSL signals were detected with a Si CCD-based spectrometer (Ocean Optics, QE Pro).⁽²⁷⁾ Each sample was heated to 400 °C at a rate of 1 °C/s to obtain TSL glow curves and spectra. For the fading property, the TSL glow curves were measured after keeping the sample for 24 h at room temperature.

The 0.5% Dy-doped sample was exposed to 1 Gy of X-rays through a Pb-based square test chart (DIAGNOMATIC, Pro-res RF BarType7) using the X-ray source to evaluate spatial resolution. After heating the 0.5% Dy-doped sample to 200 °C using a ceramic hot plate (As One, CHO-170AF), a CCD camera (Bitran Corp, BK-54DUV) was used to measure the spatial distribution of TSL. Additionally, the spatial resolution of commercial Eu-doped CsBr (Konica Minolta) was evaluated as a reference for comparison with 0.5% Dy-doped sample. A radiation dose of 1 Gy was delivered to the Eu-doped CsBr utilizing the X-ray generator and the test chart. Following the X-ray exposure, the Eu-doped CsBr was stimulated with 690 nm light using a xenon lamp (Asahi Spectra, LAX-C100), and OSL was recorded using the CCD camera.

3. Results and Discussion

The appearances and XRD patterns of the Dy-doped samples and the reference data (JCPDS 29-1301) are shown in Fig. 1. The thickness of all Dy-doped samples was approximately 1 mm. Under room light, all samples appeared visibly transparent and colorless. The XRD patterns of the prepared crystals matched the reference data, confirming that all the prepared crystals were single-phase SGPO. The ionic radii for Sr^{2+} , Gd^{3+} , and Dy^{3+} are 1.31, 0.97, and 0.92 Å, respectively.^(15,28,29) Given these values, Dy^{3+} would likely replace Gd^{3+} sites owing to their similar ionic radii and valence. Additionally, no discernible peak shift would be observed within the detection limit of this study owing to the similar ionic radii of Dy^{3+} and Gd^{3+} .

Figure 2 depicts the TSL glow curves of Dy-doped samples after the X-ray irradiation of 1 Gy and the 0.5% Dy-doped sample after the X-ray irradiation of 1 Gy after keeping the sample for 24 h under room temperature. The inset shows the curve for the nondoped sample after the X-ray irradiation of 1 Gy. The emission intensity of the samples was corrected by their mass. All the Dy-doped samples exhibited two glow peaks at 80 and 110 °C. In contrast, a single peak was observed at 70 °C in the nondoped sample in our previous investigation.⁽²³⁾ This result suggests that Dy doping creates new trapping centers with different energy levels. The 1% Dy-doped sample showed the maximum TSL intensity among the present samples. The TSL intensity typically depends on three factors: (i) the number of carriers trapped in trapping centers, (ii) the possibility of carriers being released from trapping centers through external thermal stimulation, and (iii) the emission efficiency resulting from the recombination of carriers (QY). Therefore, although the 5% Dy-doped sample had a higher PL QY than the 1% Dy-doped sample, the 1% Dy-doped sample exhibited a higher TSL intensity than the 5% Dy-doped sample because Dy doping likely caused a decrease in (i) and/or (ii). On the basis of the fading property, the TSL intensity of the 0.5% Dy-doped sample decreased to 55% for the first 24 h. The fading rate of this sample was significantly higher than those of some commercial dosimeters.⁽³⁰⁾ Therefore, the Dy-doped samples require improvement of the fading property of TSL.

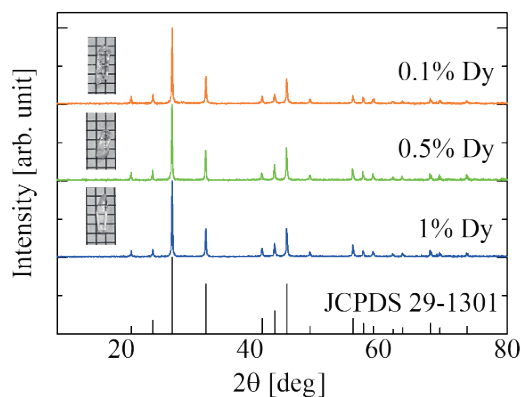


Fig. 1. (Color online) XRD patterns of Dy-doped samples (inset) and reference data (JCPDS 29-1301).

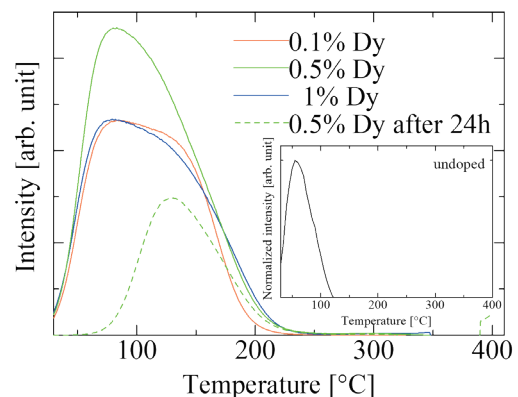


Fig. 2. (Color online) TSL glow curves of undoped (inset) and Dy-doped samples.

Since the TSL glow curves are not resolved by wavelengths, it is impossible to identify emission centers from them. Wavelength-resolved TSL measurements are required to determine emission centers of TSL. Figure 3 displays the TSL spectra of the Dy-doped samples following 1 Gy X-ray irradiation. For the measurements, all the Dy-doped samples were heated to 80 °C. The emission peaks were observed at 315–760 nm in the Dy-doped samples. The TSL peaks at 315 and 480–620 nm could result from the $4f-4f$ transitions of Gd^{3+} and Dy^{3+} , respectively.^(31–35) A comparison of all the Dy-doped samples showed that the intensity ratio of the emission of Gd^{3+} to that of Dy^{3+} changes with the increase in Dy concentration. The reason considered is that as the Dy concentration increased, the probability of energy transfer from Gd to Dy increased.⁽³⁶⁾ Figure 4 shows the TSL intensity profile perpendicular to the line pattern (6.30 and 8.90 LP/mm) along with the X-ray image of the 0.5% Dy-doped sample. X-ray images were obtained immediately after the X-ray irradiation of 1 Gy. Five peaks were observed in the intensity profile at the 6.30 and 8.90 LP/mm sections. However, no peaks were detected in the intensity profile at sections with spatial resolution higher than 8.90 LP/mm. Therefore, it was concluded that the 0.5% Dy-doped sample had a spatial resolution of 8.90 LP/mm. The five peaks of 8.90 LP/mm sections appeared a little noisy. The reason would be cracks in the sample. The inset of Fig. 4 shows the OSL intensity profile perpendicular to the line pattern (1.25 and 1.80 LP/mm) along with the X-ray image of Eu-doped CsBr. In the intensity profile at the 1.25 and 1.80 LP/mm sections, five peaks were observed. However, no peaks were detected in sections with spatial resolutions higher than 1.80 LP/mm. The results suggest that the Eu-doped CsBr had a 1.80 LP/mm spatial resolution. The line widths on each X-ray test chart were 1.25, 1.80, 6.30, and 8.90 LP/mm (400, 278, 79.4, and 56.2 μm , respectively). A comparison between the Eu-doped CsBr and the 0.5% Dy-doped sample confirmed that the 0.5% Dy-doped sample exhibited a superior spatial resolution when evaluated using commercially available machines. The reason why Dy-doped samples exhibited high spatial resolutions is that the single crystals allowed luminescence to be observed from deep within the samples, which positively contributed to the emission intensity.

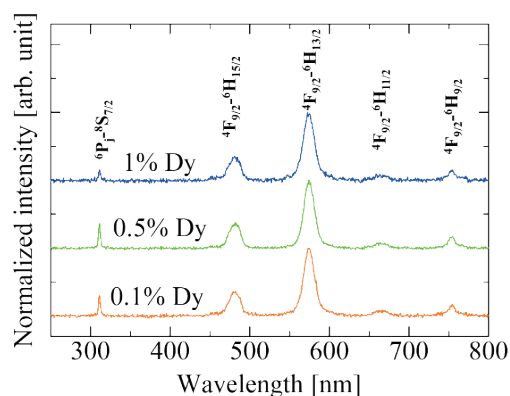


Fig. 3. (Color online) TSL spectra of Dy-doped samples after 1 Gy X-ray exposure.

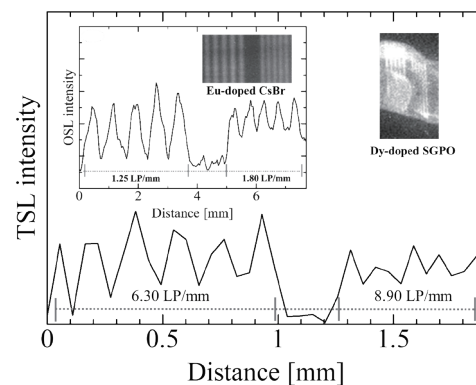


Fig. 4. (Color online) X-ray images and intensity profiles perpendicular to line patterns of 0.5% Dy-doped sample and Eu-doped CsBr.

4. Conclusions

The FZ method was used to grow Dy-doped SGPO single crystals. As indicated by powder XRD patterns, all the prepared samples were single-phase SGPO. The emission peaks at 480–760 nm attributed to Dy³⁺ 4f–4f transitions were observed in TSL spectra. All the samples displayed TSL glow peaks at 80 and 110 °C. Furthermore, the 0.5% Dy-doped sample demonstrated a 56.2 μm spatial resolution when exposed to 1 Gy of X-ray radiation.

Acknowledgments

This work was supported by MEXT Grants-in-Aid for Scientific Research A (22H00309), Scientific Research B (23K21827, 23K25126 and 24K03197), Exploratory Research (22K18997), and Early-Career Scientists (23K13689), and the Cooperative Research Project of Research Center for Biomedical Engineering, Nippon Sheet Glass Foundation, Terumo Life Science Foundation, KRF Foundation, Tokuyama Science Foundation, Iketani Science and Technology Foundation, Iwatani Naoji Foundation, and Foundation for Nara Institute of Science and Technology.

References

- 1 D. Mouhssine, A. Nourredine, A. Nachab, A. Pape, and F. Fernandez: Nucl. Instrum. Methods Phys. Res. B **227** (2005) 609. <https://doi.org/10.1016/j.nimb.2004.10.078>
- 2 T. Kato, D. Nakauchi, N. Kawaguchi, and T. Yanagida: Jpn. J. Appl. Phys. **62** (2023) 010604. <https://doi.org/10.35848/1347-4065/ac94ff>
- 3 T. Yanagida, G. Okada, and N. Kawaguchi: J. Lumin. **207** (2019) 14. <https://doi.org/10.1016/j.jlumin.2018.11.004>
- 4 D. Shiratori, H. Fukushima, D. Nakauchi, T. Kato, N. Kawaguchi, and T. Yanagida: Jpn. J. Appl. Phys. **62** (2023) 010608. <https://doi.org/10.35848/1347-4065/ac90a4>
- 5 K. Shinsho, R. Oh, M. Tanaka, N. Sugioka, H. Tanaka, G. Wakabayashi, T. Takata, W. Chang, S. Matsumoto, G. Okada, S. Sugawara, E. Sasaki, K. Watanabe, Y. Koba, K. Nagasaka, S. Yoshihashi, A. Uritani, and T. Negishi: Jpn. J. Appl. Phys. **62** (2023) 010502. <https://doi.org/10.35848/1347-4065/ac971e>
- 6 H. Kimura, T. Kato, T. Fujiwara, M. Tanaka, D. Nakauchi, N. Kawaguchi, and T. Yanagida: Jpn. J. Appl. Phys. **62** (2023) 010504. <https://doi.org/10.35848/1347-4065/ac916c>
- 7 G. Okada, Y. Koguchi, T. Yanagida, S. Kasap, and H. Nanto: Jpn. J. Appl. Phys. **62** (2023) 010609. <https://doi.org/10.35848/1347-4065/ac9023>
- 8 D. Shiratori, H. Kimura, Y. Fukuchi, and T. Yanagida: Sens. Mater. **36** (2024) 547. <https://doi.org/10.18494/SAM4764>
- 9 H. Ezawa, Y. Takebuchi, T. Kato, D. Nakauchi, N. Kawaguchi, and T. Yanagida: Jpn. J. Appl. Phys. **62** (2023) 122001. <https://doi.org/10.35848/1347-4065/ad0a46>
- 10 H. Ezawa, Y. Takebuchi, K. Ichiba, T. Kato, D. Nakauchi, N. Kawaguchi, and T. Yanagida: Opt. Mater. **147** (2024) 114665. <https://doi.org/10.1016/j.optmat.2023.114665>
- 11 B. Marczevska, P. Bilski, D. Wróbel, and M. Kłosowski: Radiat. Meas. **90** (2016) 265. <https://doi.org/10.1016/j.radmeas.2016.02.004>
- 12 C. B. Palan, N. S. Bajaj, A. Soni, and S. K. Omanwar: J. Lumin. **176** (2016) 106. <https://doi.org/10.1016/j.jlumin.2016.03.014>
- 13 H. Ezawa, Y. Takebuchi, K. Okazaki, T. Kato, D. Nakauchi, N. Kawaguchi, and T. Yanagida: J. Mater. Sci.: Mater. Electron. **35** (2024) 238. <https://doi.org/10.1007/s10854-024-11995-w>
- 14 H. Ezawa, Y. Takebuchi, K. Okazaki, T. Kato, D. Nakauchi, N. Kawaguchi, and T. Yanagida: Sens. Mater. **36** (2024) 465. <https://doi.org/10.18494/SAM4757>
- 15 Z. Yang, D. Xu, J. Sun, Y. Sun, and H. Du: Opt. Eng. **54** (2015) 105102. <https://doi.org/10.1117/1.OE.54.10.105102>
- 16 Q. Xu, J. Sun, D. Cui, Q. Di, and J. Zeng: J. Lumin. **158** (2015) 301. <https://doi.org/10.1016/j.jlumin.2014.10.034>

- 17 R. Tsubouchi, H. Fukushima, T. Kato, D. Nakauchi, S. Saijo, T. Matsuura, N. Kawaguchi, T. Yoneda, and T. Yanagida: *Sens. Mater.* **36** (2024) 481. <https://doi.org/10.18494/SAM4763>
- 18 S. Otake, H. Sakaguchi, Y. Yoshikawa, T. Kato, D. Nakauchi, N. Kawaguchi, and T. Yanagida: *Sens. Mater.* **36** (2024) 539. <https://doi.org/10.18494/SAM4759>
- 19 T. Kato, H. Kimura, K. Okazaki, D. Nakauchi, N. Kawaguchi, and T. Yanagida: *Sens. Mater.* **35** (2023) 483. <https://doi.org/10.18494/SAM4137>
- 20 K. Ichiba, Y. Takebuchi, H. Kimura, T. Kato, D. Nakauchi, N. Kawaguchi, and T. Yanagida: *Sens. Mater.* **35** (2023) 475. <https://doi.org/10.18494/SAM4143>
- 21 H. Nanto and G. Okada: *Jpn. J. Appl. Phys.* **62** (2023) 010505. <https://doi.org/10.35848/1347-4065/ac9106>
- 22 H. Kawamoto, M. Koshimizu, Y. Fujimoto, and K. Asai: *Jpn. J. Appl. Phys.* **62** (2023) 010501. <https://doi.org/10.35848/1347-4065/ac9cb0>
- 23 E. Haruaki, Y. Takebuchi, K. Okazaki, K. Ichiba, T. Kato, D. Nakauchi, N. Kawaguchi, and T. Yanagida: *Radiat. Phys. Chem.* **220** (2024) 111721. <https://doi.org/10.1016/j.radphyschem.2024.111721>
- 24 E. Aşlar: *Radiat. Meas.* **154** (2022) 106779. <https://doi.org/10.1016/j.radmeas.2022.106779>
- 25 T. Kato, D. Nakauchi, N. Kawaguchi, and T. Yanagida: *Opt. Mater.* **132** (2022) 112785. <https://doi.org/10.1016/j.optmat.2022.112785>
- 26 D. Nakauchi, G. Okada, N. Kawaguchi, and T. Yanagida: *Jpn. J. Appl. Phys.* **57** (2018) 100307. <https://doi.org/10.7567/JJAP.57.100307>
- 27 G. Okada, T. Kato, D. Nakauchi, K. Fukuda, and T. Yanagida: *Sens. Mater.* **28** (2016) 897. <https://doi.org/10.18494/SAM.2016.1357>
- 28 Q. Liu, Y. Liu, Y. Ding, Z. Peng, X. Tian, Q. Yu, and G. Dong: *Ceram. Int.* **40** (2014) 10125. <https://doi.org/10.1016/j.ceramint.2014.01.137>
- 29 J. Sokolnicki and E. Zych: *J. Lumin.* **158** (2015) 65. <https://doi.org/10.1016/j.jlumin.2014.09.033>
- 30 J. A. Harvey, N. P. Haverland, and K. J. Kearfott: *Appl. Radiat. Isot.* **68** (2010) 1988. <https://doi.org/10.1016/j.apradiso.2010.04.028>
- 31 S. Liu, M. Lv, J. Zhou, Y. Zhu, R. Hu, X. Li, and D. Xu: *Optik (Stuttg)* **281** (2023) 170833. <https://doi.org/10.1016/j.jjleo.2023.170833>
- 32 K. Chalvan, D. N., H. C. Manjunatha, Y. S. Vidya, R. Munirathnam, S. Manjunatha, M. Shivanna, S. Kumar, E. Krishnakanth, K. Manjunatha, and S. Y. Wu: *Mater. Today Sustainability* **26** (2024) 100778. <https://doi.org/10.1016/j.mtsust.2024.100778>
- 33 A. Amarnath Reddy, M. Chandra Sekhar, K. Pradeesh, S. Surendra Babu, and G. Vijaya Prakash: *J. Mater. Chem. C* **46** (2011) 2018. <https://doi.org/10.1007/s10853-010-4851-3>
- 34 S. S. Babu, P. Babu, C. K. Jayasankar, Th. Tröster, W. Sievers, and G. Wortmann: *Opt. Mater.* **31** (2009) 624. <https://doi.org/10.1016/j.optmat.2008.06.019>
- 35 F. Nakamura, T. Kato, G. Okada, N. Kawano, N. Kawaguchi, K. Fukuda, and T. Yanagida: *Mater. Res. Bull.* **98** (2018) 83. <https://doi.org/10.1016/j.materresbull.2017.09.058>
- 36 D. Yodkantee, A. Prasatkhetragarn, N. Wantana, N. Chanthima, P. Kidkhunthod, S. Kothan, R. Yimnirun, H. J. Kim, and J. Kaewkhao: *Radiat. Phys. Chem.* **209** (2023) 110987. <https://doi.org/10.1016/j.radphyschem.2023.110987>